On the Trapping of Bjerrum Defects in Ice I_h: The Case of the Molecular Vacancy

Maurice de Koning* and Alex Antonelli

Instituto de Física "Gleb Wataghin", Universidade Estadual de Campinas, 13083-970, Campinas − SP, Brazil

Received: July 19, 2007; In Final Form: August 30, 2007

We present a density-function theory (DFT) study of Bjerrum-defect trapping centers involving the molecular vacancy in ice I_h. As a first step, we compute the intrinsic migration barrier to D-defect motion using the nudged elastic band (NEB) method and find them to be of the same order of magnitude as the energy barriers involving intrinsic L-defect motion. This finding suggests that intrinsic mobility factors cannot explain the experimentally observed inactivity of D defects, supporting the idea that D defects are trapped at other lattice-defect sites. Next we study the defect complexes formed by the combination of isolated D and L defects with a molecular vacancy. The corresponding geometries show that the formation of these aggregates significantly reduces elastic distortions that are present in isolated Bjerrum defects. An analysis of the energetics involved in the formation of both defect complexes reveals a significant binding energy, indicating that the molecular vacancy represents a strong trapping center for Bjerrum defects. On the other hand, the fact that there is no difference between the absolute values of the binding energies for both D and L defects suggests that the vacancy affects both species of Bjerrum defects in a similar fashion, possibly ruling out the vacancy trapping centers as an explanation for the experimentally observed inactivity of D defects.

1. Introduction

Although the isolated water molecule is one of the simplest in chemistry and is generally well-understood, the condensed phases of water display a remarkably rich panorama of properties that still elude satisfactory comprehension. This complexity is reflected, for instance, in water's phase diagram, which, aside from the liquid state, contains at least 9 distinct stable crystalline phases.[1] Although the transitions between the different phases are among the issues that have yet to be elucidated, not even the properties of the individual states may be claimed to have been fully resolved. The proton-disordered hexagonal crystalline phase of water, ice I_h, which is one of the most abundant crystalline materials on Earth, represents a notable example. Although several decades of experimental and theoretical studies have unequivocally demonstrated that crystal defects play a fundamental role in the properties of ice I_h,[1] a consistent and quantitative interpretation of all of the observed effects in terms of defect behavior is still lacking.

Ice I_h is characterized by a structure in which the water molecules are arranged on a Wurtzite hexagonal lattice, each water molecule being surrounded by 4 nearest neighbors located at the corners of a regular tetrahedron.[1] In addition to these crystallographic characteristics, an essential feature of the ice I_h structure is the lack of long-range order in the orientation of the water molecules on their lattice sites. These structural features can be summarized in terms of the two Bernal−Fowler ice rules:[1,2] (i) each molecule accepts/donates two protons from/to two nearest-neighbor molecules and (ii) there is precisely one proton between each nearest-neighbor pair of oxygen atoms. A typical structure is shown in Figure 1, which depicts a view of the defect-free ice I_h structure along a direction close to that of the *c* axis.

Considering the issue involving the relationship between the observed macroscopic properties and the characteristics of intrinsic crystal defects, the peculiar electrical properties of ice I_h represent a case of particular interest. When a specimen is subjected to a static external electric field *E*, for instance, the ice responds by electric polarization, both through the polarization of the charge distribution within the individual molecules as well as by the reorientation of molecular dipole moments as a whole. The latter contribution is a relatively slow process in which the approach of the electric polarization *P* to its equilibrium value P_s is described by[1]

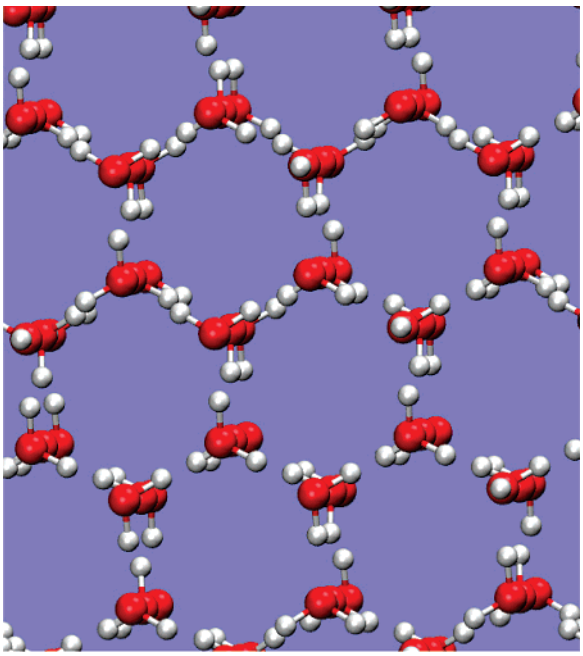

Figure 1. Schematic representation of the ice I_h crystal structure. The red spheres represent oxygen atoms, which occupy the sites of a Wurtzite hexagonal lattice structure. The white spheres depict the protons. The view is along a direction close to that of the *c* axis.

* Corresponding author. E-mail: dekoning@ifi.unicamp.br.

10.1021/jp075661y CCC: $37.00
Published on Web 10/11/2007

$$\frac{dP}{dt} = \frac{1}{\tau_D}(P_s - P) \quad (1)$$

where τ_D is the Debye relaxation time. The nature of the electrical polarization in the liquid phase of water is essentially the same as that in ice. However, there is an enormous disparity in the time scales τ_D associated with molecular-dipole realignments. Whereas the typical Debye relaxation time in ice I_h at a temperature of $T = -10$ °C is of the order of $\tau_D \cong 10^{-5}$ s, its value in liquid water at $T = +10$ °C is approximately 6 orders of magnitude shorter, $\tau_D \cong 10^{-11}$s. This tremendous difference is due to the fact that, compared to the liquid state, it is much more difficult for the molecules to reorient themselves in the crystalline phase due to their bonding in the lattice and the Bernal−Fowler ice rules. In fact, in an ice crystal in which both ice rules are strictly obeyed, the molecular-dipole realignments would not be possible at all, given that the orientation of a given molecule is then strictly determined by its neighbors.

This observation led Bjerrum[3] to postulate the existence of intrinsic lattice imperfections, referred to as protonic defects, that constitute local violations of the ice rules and whose thermally activated motion provokes molecular reorientations. This idea is also consistent with the experimental fact that the temperature-dependence of the time scale τ_D follows essentially an Arrhenius-type law, the same kind that generally characterizes the thermodynamic properties of intrinsic lattice defects in crystalline solids.

The class of protonic defects in ice I_h consists of two pairs of lattice imperfections, each representing a violation of one of the ice rules. The creation of both defect pairs is depicted schematically in Figure 2, in which we show a two-dimensional square ice[1] representation to facilitate visualization. Figure 2a shows the two-dimensional representation of defect-free ice, in which each molecule donates/receives two protons to/from its 4 nearest-neighbor molecules. The first protonic defect pair, which corresponds to a violation of the first ice rule, is then created by transferring a proton from a given molecule to a neighboring one, inverting the proton acceptor/donor status of both molecules, and leading to the creation of an embryonic OH^-/H_3O^+ ionic defect pair. Further proton-transfer events can further separate both ions, eventually creating independent OH^- and H_3O^+ defects. The second type of protonic defect pair, referred to as the Bjerrum defect pair, embodies the violation of the second ice rule. It is created by the rotation of a water molecule such that one of the nearest-neighbor oxygen−oxygen "bonds" is occupied by two protons, referred to as a D defect, and another, named an L defect, is left without any protons. This process is depicted schematically in Figure 2c. Similar to the case of the ionic defect pair, successive molecular rotations can further separate the Bjerrum-defect pair, eventually creating independent D and L defects. The detailed molecular structure of the D and L defects, however, is somewhat different from the schematic picture shown in Figure 2. In the case of the D defect, for instance, a situation with two protons located along the line between two nearest-neighbor oxygen atoms is highly unstable due to the strong electrostatic repulsion. As a result, one of the protons rotates away from the line, leaving a dangling proton and a distorted hydrogen bond.[4−6]

Subsequently, Jaccard[1,7] developed a quantitative theory describing the macroscopic dielectric polarization and electrical conductivity properties of ice in terms of the concentrations, mobilities, and the effective charges of the D and L Bjerrum defects and the H_3O^+ and OH^- ionic defects. Since it provides a direct link between the microscopic structural characteristics

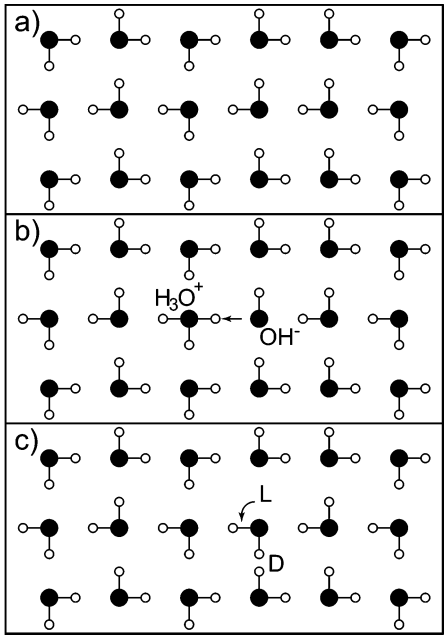

Figure 2. Schematic representation of protonic defect formation in two-dimensional square ice. (a) Defect-free ice. (b) Formation of ionic OH^-/H_3O^+ defect pair through proton transfer. (c) Creation of embryonic D/L Bjerrum defect-pair.

of ice and its macroscopic electric properties, Jaccard's theory has been used to interpret experimental observations in terms of the properties of the individual Bjerrum and ionic defects. Despite the difficulties involved in some of the interpretations,[1] the series of experiments carried out over the past 50 years[1,7−9] have led to a fairly complete picture of the fundamental parameters describing the energetics and effective charges carried by Bjerrum and ionic defects.[10]

A notable exception involves the migration energetics of the D defect, for which no quantitative experimental estimates are available. This is closely related to the apparent asymmetry in the roles of both Bjerrum-defect species as far as their mobility is concerned. Although the intrinsic (thermal equilibrium) concentrations of D and L defects need to be equal,[1] the D defect is found to be much less mobile than its L counterpart. In fact, not even in doped ice, in which an extrinsic (athermal) concentration of D defects may be expected to be present, has there been any reliable evidence for D-defect mobility,[1,11,12] preventing the experimental determination of D-defect migration barriers. This observation has led to the idea that, in the absence of intrinsic mobility issues, D defects may be trapped at other lattice defect sites.[1,13−15]

Although the character of these trapping centers remains unknown, experimental data on the solvated electron in ice point toward the molecular vacancy as a potential candidate.[15,16] The corresponding defect complex, which results from the combination of a D defect and a molecular vacancy (V) is depicted schematically in Figure 3, using the two-dimensional square ice representation for visualization. Figure 3a shows the presence of separate D and L defects, as well as a molecular vacancy. The latter is characterized by the lack of a water molecule on a given lattice site, resulting in a cavity that has two protons pointing inward. In Figure 3b, a D defect has combined with a molecular vacancy, resulting in the positively vested vacancy (DV) structure that features a cavity having 3 protons pointing inward. The conceptual resemblance of this structure with the Kevan structure of the solvated electron in liquid water[16] and the similarity of the optical absorption spectra of the solvated

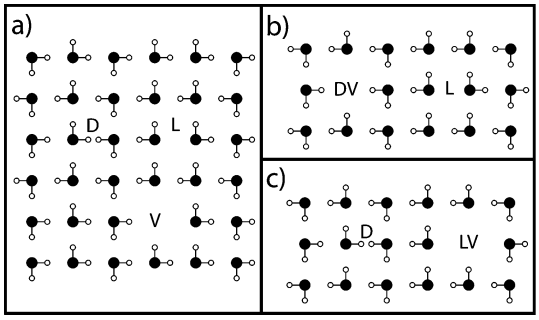

Figure 3. Schematic representation of defect complexes involving the combination of a D or L Bjerrum defect with a lattice vacancy. (a) Individual D and L defects and molecular vacancy. (b) Combination of D defect with a molecular vacancy, referred to as the DV complex. The structure features a cavity with three inward-pointing protons. (c) Combination of L defect with a molecular vacancy, referred to as the LV complex. The structure is characterized by a cavity with only a single inward-pointing proton.

electron in liquid water and ice[17−20] has led to the hypothesis of a significant thermal-equilibrium presence of DV defects in ice. This would then be consistent with a picture in which a significant fraction of D defects is trapped at molecular vacancies, possibly explaining the observed inactivity of D defects in electrical conductivity/dielectric polarization experiments in ice.

The latter implication, however, appears valid only if the interaction with the molecular vacancy were to be significantly different for D and L defects. Only if the former were found to be strongly trapped at the vacant lattice site whereas the latter is not would the DV trapping center provide a plausible explanation for the observed D-defect inactivity. In this light, a comparison between the DV center and the LV defect complex, which is formed by combining an L defect with a lattice vacancy and is characterized by a cavity with only a single inward-pointing proton, as shown schematically in Figure 3c, is imperative. Such a comparison is the objective of the present work, in which we utilize density-functional-theory (DFT) calculations[21] to examine the intrinsic mobility of D defects, as well as the structure and energetics of the DV and LV defect aggregates in ice I_h.

The remainder of this paper has been organized as follows. In section 2, we describe the details of the employed computational methods. The obtained results are described and discussed in section 3, which is followed by a summary and conclusions in section 4.

2. Computational Details

2.1. Computational Cell. All of the calculations have been carried out using a supercell containing 96 water molecules subject to periodic boundary conditions. The defect-free cell, as developed by Hayward and Reimers,[22] features a proton-disordered ice I_h structure strictly satisfying the Bernal−Fowler ice rules and having a zero net dipole moment. Starting from this defect-free geometry, several different defect cells were created to represent, respectively, a single molecular vacancy (V), an isolated D/L Bjerrum defect pair (DL), a DV defect complex plus an isolated L defect (DV + L), and an LV aggregate plus and isolated D defect (LV + D). To compute binding energies of the DV and LV defect aggregates, the vacancy was introduced at the same lattice site in both the isolated-vacancy cell as well as the corresponding DV + L and LV + D defect cells. Furthermore, to probe the possible influence of the proton-disordered character on the defect energetics, several different realizations of each defect type were created, introducing the defects in question at different locations in the original defect-free cell.

2.2. Density Functional Theory Calculations. All computations have been carried out using density functional theory (DFT) within the generalized-gradient approximation (GGA), as implemented in the VASP package.[23−26] Following previous studies involving ice I_h,[6,27] we utilized the Perdew−Wang 91 functional to describe exchange-correlation effects and employed the projected-augmented-wave (PAW) approach.[28] Brillouin-zone sampling was limited to the Γ point, and the Kohn−Sham orbitals were expanded using a plane-wave basis set with a kinetic-energy cutoff of 700 eV. After their initial creation, all defect structures were relaxed by minimizing the magnitude of the Hellmann−Feynman forces to a level below a tolerance of 0.01 eV/Å.

2.3. Determination of Migration Barriers. To investigate the intrinsic mobility of isolated D defects, we computed the migration barriers using the nudged elastic band (NEB) method augmented with the climbing image approach[29] to locate saddle points between two adjacent stable equilibrium configurations of the D defect. The method was employed using 4 intermediate images along the path and a spring constant of 5.0 eV/Å^2.

3. Results and Discussion

3.1. Intrinsic D-Defect Mobility. As pointed out in the Introduction, the need for a hypothesis in which other lattice defects are held responsible for the observed inactivity of D defects relative to L defects in molecular reorientation processes is based on the assumption that there are no significant differences in the intrinsic mobilities of D and L defects, i.e., the mobilities of single, isolated D and L defects in otherwise defect-free ice I_h surroundings. Indeed, previous molecular dynamics (MD) simulations based on empirical water potentials[4,5] seem to point in this direction, suggesting that there are no factors associated with the underlying I_h lattice structure that might cause such a fundamental difference between the two.

In a recent study,[6] we computed the migration energy barrier for L defects, using precisely the same first-principles approach adopted in the present work. Sampling 6 different L-defect hopping events, the intrinsic L-defect migration barrier was found to range between 0.10 and 0.14 eV, in which the fluctuations are due to the proton-disordered character of the ice I_h lattice structure. These values were found to be consistent with the mentioned empirical MD studies, indicating an overall high intrinsic mobility of L defects. The corresponding experimental value[1] ranges between 0.2 and 0.3 eV. As discussed elsewhere,[6] the discrepancies between the theoretical and the experimental values for the L-defect migration barriers are likely to be a result of the large experimental uncertainties associated with the fact that the L-defect mobility can only be determined indirectly, requiring interpretation of experiments carried out using doped ice samples.[1]

To complete the picture of the intrinsic mobilities within the present level of modeling, we computed the migration barriers for D defect motion. To this end, we created a number of defect cells containing an isolated D/L defect pair by a series of molecular rotations of the type shown schematically in Figure 2c, followed by geometry optimization. On the basis of these relaxed defect cells, we created new ones in which the D-defect position had been modified with respect to the original cell by means of a single molecular rotation, again followed by structural relaxation. Taking the cells with the structures before and after the D-defect hop as beginning and end points, we used

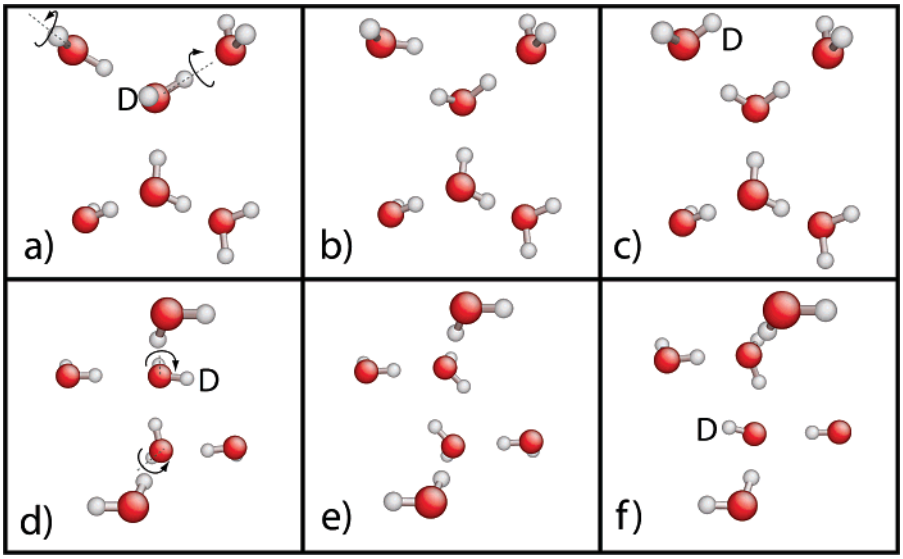

Figure 4. Mechanisms of D-defect motions as determined using the NEB method. Panels a−c show the progress of a D-defect hop in case the rotation axes of the original and new host molecules are close to perpendicular (87°). Panel c represents the saddle-point configuration. Panels d−f show a second case, in which the rotation axes are nearly parallel (11°). Panel e shows the saddle-point configuration.

the NEB method to locate a saddle point between then and determine the corresponding migration barrier.

The energy barrier associated with intrinsic D-defect motion appears to depend on the orientation of the molecules in the immediate vicinity of the D defect. This is illustrated in Figure 4, which shows the initial (panels a and d) and final equilibrium structures (panels c and f) of the D defect, as well as the corresponding saddle-point configurations (panels b and e) for two distinct cases. In the first case, shown in panels a−c, the migration energy is found to be relatively high. The motion of the D defect proceeds by rotation of the hosting molecule about the axis pointing along the hydrogen-bonded O−H bond of the hosting molecule. The depicted rotation then induces the rotation of one of its nearest-neighbor molecules, which becomes the new host of the D defect, as shown in panel c. In this particular case, however, the axis about which the original host molecule rotates is very nearly perpendicular (87°) to the rotation axis of the new host. In purely geometrical and rigid-body terms, this suggests that the torque with respect to the rotation axis of the new host due to the original one may be expected to be relatively small. A different case is shown in panels d−f, where the angle between both rotation axes is only 11°, so that the torque with respect to the rotation axis of the new host should be significantly larger than in the previous situation. Indeed, the NEB results for a set of 4 rotation axis pairs are consistent with such a correlation, as is shown in Figure 5. For each angle, there are two migration-energy barrier values, corresponding to the forward and backward D-motion events respectively. Due to the proton-disordered character of the ice I_h structure, these barriers are in general different, with fluctuations of the order of 0.01 eV, which is consistent with previous calculations.[6,26] The observation that the migration barrier depends on the orientation of the molecules in the immediate vicinity of the D defect may possibly be related to there existing two different classes of hydrogen bonds, either parallel to the *c* axis or in the *ab* plane, which provide a different orientational relationship between connected tetrahedra.[30]

A more important implication of the results shown in Figure 5 in the present context, however, is that the migration barrier to intrinsic D-defect motion does not appear to be larger than that associated with intrinsic L-defect motion,[6] suggesting that the observed inactivity of D defects in molecular reorientation

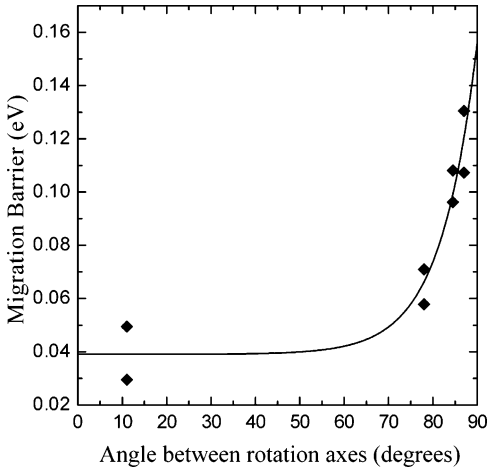

Figure 5. D-defect migration barrier as a function of angle between the rotation angle of original and new host molecule. Each pair of rotation angles yields two values for the migration barrier, corresponding to the forward and backward migration events, respectively.

processes cannot be explained in terms of intrinsic mobility factors, supporting the idea of trapping centers involving other defects.

3.2. Formation Energetics of DV and LV Defect Aggregates. Having considered intrinsic mobility factors, we now turn to the structural and energetic properties of Bjerrum-defect trapping sites involving single molecular vacancies. In this light, we analyze both the positively and negatively vested vacancies, which are formed by the combination of an L defect with a vacancy (LV) and a D defect with a molecular vacancy (DV), respectively. Figure 6 depicts typical molecular structures involved in the formation of both defect complexes. Panel a shows the relaxed structure an isolated L defect, in which the two nearest-neighbor molecules hosting the L defects are indicated by the arrows. As reported earlier,[4−6] the L defect involves a significant local distortion of the ice I_h lattice, increasing the nearest-neighbor distance of the pair of oxygen atoms between which a proton is missing by almost 25% with respect to the defect-free lattice value. Panel b now shows the structure that results when a vacancy is introduced at the L defect, removing the molecule indicated by the left arrow in panel a. Clearly, the introduction of the vacancy results in a

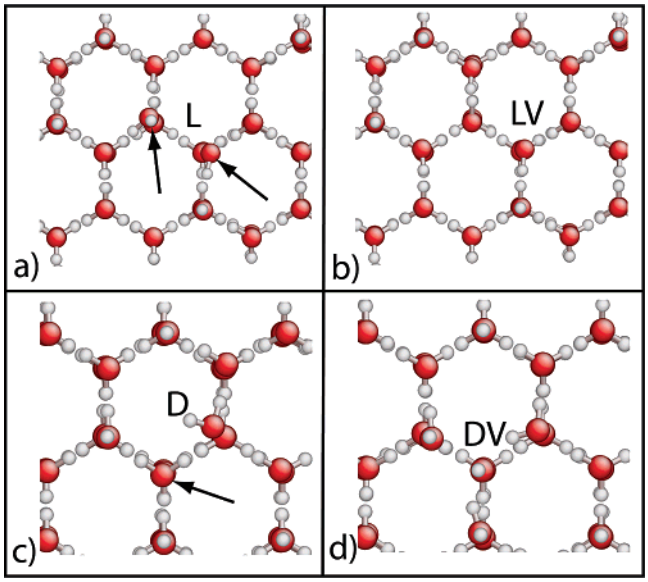

Figure 6. Typical molecular structures involved in the formation of the LV and DV defect complexes. Panel a shows the typical molecular structure of an isolated L defect, in which the distance between the two hosting molecules, indicated by the two arrows, shows a significant increase with respect to the defect-free crystal value. Panel b shows that the introduction of a molecular vacancy, by removing the molecule indicated by the left arrow creates the LV defect complex, significantly relieves the local distortions. A similar effect occurs in the formation of the DV defect complex. Panel c shows a typical molecular structure of an isolated D defect, in which the position of the host molecule is distorted significantly with respect to its defect-free lattice position. Panel d) depicts the creation of the DV defect complex, which is produced by removing the molecule indicated by the arrow in panel c. The relaxed structure of the DV defect reveals a significant relief of the distortions present in the isolated D defect.

significant relief of the lattice distortion, with the remaining molecule hosting the original L defect almost returning to its defect-free lattice site. A similar effect occurs for the DV defect complex, as can be seen in panels c and d. The former shows an isolated D defect, featuring rather large distortions of the hosting molecule, the introduction of a molecular vacancy, created by removing the molecule indicated with the arrow in panel c, again leads to a substantial relaxation of the local strain.

The relief of the local lattice distortions is reflected in the formation energetics of the LV and DV defect complexes. To quantify this effect, we compute the binding energy ΔE_b of both defect aggregates, considering a number of different realizations to probe the magnitude of the fluctuations due to the proton-disordered character of the ice I_h structure. The binding energies of the defect complexes are defined according to

$$\Delta E_b^{LV} = \Delta E_{LV+D} - (\Delta E_{DL} + \Delta E_V) \quad (2)$$

and

$$\Delta E_b^{DV} = \Delta E_{DV+L} - (\Delta E_{DL} + \Delta E_V) \quad (3)$$

where ΔE_{LV+D}, ΔE_{DV+L}, ΔE_{DV}, and ΔE_V represent the formation energies of the LV + D, DV + L, D + L, and V defect cells, respectively. As is customary, all formation energies are measured with respect to the reference energy of a defect-free cell containing the same number of molecules. Table 1 shows the corresponding values for three different realizations of the DV and LV defect complexes.

The results show significantly negative binding energies for both defect complexes. The fact that the binding energies are

TABLE 1: Formation and Binding Energies of DV and LV Defect Complexes in Ice I_h[a]

realization	ΔE_{DL} (eV)	ΔE_V (eV)	$\Delta E_{DV(LV)+L(D)}$ (eV)	ΔE_b (eV)	$\overline{\Delta E_b}$ (eV)
DV1	1.198	0.730	1.384	−0.544	−0.55 ± 0.01
DV2	1.234	0.711	1.379	−0.566	
DV3	1.219	0.701	1.379	−0.541	
LV1	1.198	0.712	1.358	−0.552	−0.55 ± 0.01
LV2	1.214	0.759	1.411	−0.562	
LV3	1.085	0.731	1.279	−0.537	

[a] The final column shows the respective average as computed from the three distinct realizations.

negative indicates that there is an energy gain upon the formation of the Bjerrum-defect/vacancy complex, compared to a situation with isolated Bjerrum defects and an isolated molecular vacancy. Furthermore, given that the magnitude of the binding energies is so high, being close to the sublimation energy of around 0.6 eV per molecule,[1] indicates that the molecular vacancy indeed represents a deep trapping center for Bjerrum defects. On the other hand, although supporting the view that the molecular vacancy represents a deep trap to D defects, the results in Table 1 also suggest that this trapping center cannot explain the observed asymmetry in the activity of Bjerrum defects in the processes involving molecular reorientations. Although the experimental evidence clearly indicates an inactivity of D defects relative to L defects, the present results do not show any such asymmetry, giving essentially equal average binding energies for both the DV and DL defect complexes. This implies that molecular vacancies are expected to trap D and L defects in a similar fashion, apparently ruling them out as the cause of the observed inactivity of D defects.

4. Summary and Conclusions

In this paper, we contemplate the issue involving the experimentally observed asymmetry in the behavior of D and L Bjerrum defects in dielectric polarization and electric conduction processes. Although there is ample experimental manifestation for an active role of the latter, there is no reliable evidence for any activity of the former. Assuming the absence of any intrinsic mobility differences between D and L defects, this asymmetry has led to the belief that D defects are trapped at other defect sites. The positively vested vacancy, which is formed by the combination of a D defect and a molecular vacancy, has been regarded as the most likely candidate for such a trapping center. With the purpose of analyzing the trapping potential of the vacancy, we conducted a first-principles study of the structure and energetics involved in the trapping of Bjerrum-defects at molecular vacancies in ice I_h. Our approach is based on density-functional theory within the GGA approximation,[21] the PAW approach,[28] and a plane-wave basis set, as implemented in the state-of the art package VASP,[23−26] and we utilize a 96-molecule periodic computational cell.

Before focusing on the trapping centers, we first considered the intrinsic mobility of D defects in ice I_h to evaluate the extent to which intrinsic mobility factors might play a role in the observed asymmetry. Using the nudged elastic-band method,[29] we identified a set of saddle points characterizing events in which a D defect hops from one host molecule to the next. The results indicate that, in contrast to the case of L-defect motion, the energy barrier for D-defect motion is affected significantly by the relative orientation of the original and new host molecule. The results indicate that there is a correlation between the energy-barrier value and the angle between the axes about which both molecules rotate along the hopping event. The barrier is

found to be lowest for angles close to parallel and highest for the case in which both axes are close to perpendicular. Yet, not even the highest of the located energy barriers was found to be larger than those characteristic for L defect motion. This suggests that intrinsic mobility issues cannot explain the observed D-defect inactivity in ice.

Next, we investigated the structure and energetics of defect clusters involving the combination of D and L Bjerrum defects with a molecular vacancy. For each defect complex, we considered three different realizations, creating and relaxing the defect structures in question at distinct locations in the 96-molecule periodic cell. A structural analysis of the resulting defect complexes reveals that the combination of a vacancy with the D and L Bjerrum defects leads to a significant reduction of the elastic distortions present in the isolated Bjerrum defects. This effect also manifests itself quantitatively in the binding energy of the DV and DL aggregates. It is found that the average binding energy of both defect complexes is negative, indicating a release of energy upon the combination of the Bjerrum defect and the vacancy. Computing the average values over the different realizations, it is found that the absolute values of the binding energies are essentially equal values for both DV and DL defect complexes, at a value of (0.55 ± 0.01) eV. The fact that this value is comparable to the sublimation energy in ice indicates that the vacancy indeed serves as a strong trapping center for Bjerrum defects in ice $I_{h.}$ On the other hand, the fact that both binding energies are essentially equal seems to preclude trapping centers involving the molecular vacancy as an explanation for the observed inactivity of the D defect, since they are expected to affect D and L defect in a similar fashion, in conflict with the experimental observations.

Finally, now that the molecular vacancy does not seem to be the trapping center responsible for the asymmetry in the mobility of L and D Bjerrum defects, future efforts should be targeted at other defect complexes that may serve as trapping centers. In this context, an interesting candidate involves the potential defect complexes formed by the combination of Bjerrum defects and the bond-center molecular interstitial,[27] which have been previously suggested to explain the experimental similarity of the characteristic times associated with diffusion and dielectric relaxation in ice I_h.[13]

Acknowledgment. The authors gratefully acknowledge Antônio José Roque da Silva, Adalberto Fazzio, and Robert W. Whitworth for stimulating discussions. This work was supported by the Brazilian funding agencies FAPESP and CNPq.

References and Notes

(1) Petrenko, V.; Whitworth, R. W. *Physics of Ice*; Oxford University Press: Oxford, 1999.
(2) Pauling, L. *J. Am. Chem. Soc.* **1935**, *57*, 2690.
(3) Bjerrum, N. *Science* **1952**, *115*, 385.
(4) Podeszwa, R.; Buch, V. *Phys. Rev. Lett.* **1999**, *83*, 4570.
(5) Grishina, N.; Buch, V. *J. Chem. Phys.* **2004**, *120*, 5217.
(6) de Koning, M.; Antonelli, A.; da Silva, A. J. R.; Fazzio, A. *Phys. Rev. Lett.* **2006**, *96*, 075501.
(7) Jaccard, C. *Helv. Phys. Act.* **1959**, *32*, 89.
(8) Camplin, G. C.; Glen, J. W.; Paren, J. G. *J. Glaciol.* **1978**, *21*, 123.
(9) Takei, I.; Maeno, N. *J. Phys. (Paris) Colloque C1* **1987**, *48*, 121.
(10) Hubmann, M. *Z. Phys.* **1979**, *B32*, 127.
(11) Arias, D.; Levi, L.; Lubart, L *Trans. Faraday Soc.* **1966**, *62*, 1955.
(12) Hubmann, M *J. Glaciol.* **1978**, *21*, 161.
(13) Haas, C. *Phys. Lett.* **1962**, *3*, 126.
(14) Onsager, L.; Runnels, L. K. *Proc. Natl. Acad. Sci.* **1963**, *50*, 208.
(15) Kunst, M.; Warman, J. M.; de Haas, M. P.; Verberne, J. B. *J. Phys. Chem.* **1983**, *87*, 4096.
(16) Kevan, L. *J. Phys. Chem.* **1981**, *85*, 1628.
(17) Shubin, V. N.; Zhigunov, V. A.; Zolotarevsky, V. I.; Dolin, P. I. *Nature* **1966**, *212*, 1002.
(18) Taub, I. A.; Eiben, K. *J. Chem. Phys.* **1968**, *49*, 2499.
(19) Gillis, H. A.; Quickenden, T. I. *Can. J. Chem.* **2001**, *79*, 80.
(20) Du, Y. K.; Price, E.; Bartels, D. M. *Chem. Phys. Lett.* **2007**, *438*, 234.
(21) Martin, R. M. *Electronic Structure: Basic Theory and Practical Methods*; Cambridge University Press: New York, 2004.
(22) Hayward, J. A.; Reimers, J. R. *J. Chem. Phys.* **1997**, *106*, 1518.
(23) Kresse, G.; Hafner, J. *Phys. Rev. B* **1993**, *47*, R558.
(24) Kresse, G.; Hafner, J. *Phys. Rev. B* **1994**, *49*, 14251.
(25) Kresse, G.; Furthmüller, J. *Comput. Mater. Sci.* **1996**, *6*, 15.
(26) Kresse, G.; Furthmüller, J. *Phys. Rev. B* **1996**, *54*, 11169.
(27) de Koning, M.; Antonelli, A.; da Silva, A. J. R.; Fazzio, A. *Phys. Rev. Lett.* **2006**, *97*, 155501.
(28) Kresse, G.; Joubert, D. *Phys. Rev. B* **1999**, *59*, 1758.
(29) Henkelman, G.; Uberuaga, B. P.; Jónsson, H. *J. Chem. Phys.* **2000**, *113*, 9901.
(30) Singer, S. J.; Kuo, J-L.; Hirsch, T. K.; Knight, C.; Ojamäe, L.; Klein, M. L. *Phys. Rev. Lett.* **2005**, *94*, 135701.